Zoosyst. Evol. 101 (2) 2025, 597–608 | DOI 10.3897/zse.101.133734

PENSOFT

für Naturkunde MUSEUM FÜR NATURKUNDE BERLIN

Molecular phylogeny and taxonomy of the genus *Eozapus* (Mammalia, Rodentia, Zapodidae) with the description of a new species

Siyu Yang[1], Fei Xie[1], Chengxin Zhou[1], Zongyun Zhang[1], Xuming Wang[2], Shaoying Liu[2], Shunde Chen[1]

1 *School of Life Sciences, Sichuan Normal University, Chengdu, Sichuan, 610101, China*

2 *Sichuan Academy of Forestry, Chengdu, Sichuan, 610081, China*

https://zoobank.org/FC6276C1-4634-4400-8567-CB843C5809CE

Corresponding authors: Shaoying Liu (shaoyliu@163.com); Shunde Chen (csd111@126.com)

Academic editor: Melissa T. R. Hawkins ♦ **Received** 2 August 2024 ♦ **Accepted** 4 December 2024 ♦ **Published** 10 March 2025

Abstract

Eozapus is a monotypic genus in the family Zapodidae, with a single species and two subspecies: *Eozapus setchuanus setchuanus* and *Eozapus setchuanus vicinus* in the mountains of southwestern China. *Eozapus setchuanus* is one of the oldest and rarest species. The molecular phylogenetic and evolutionary history of this species has not yet been explored because of its small size and difficulty in capturing it. In this study, we collected 51 specimens, sequenced one mitochondrial gene and two nuclear genes, and conducted morphological analyses to clarify the phylogenetic relationship and evolutionary history of this genus. Both molecular and morphological analyses supported the classification of these three species within the genus *Eozapus*. We describe a new species, *Eozapus wanglangensis* **sp. nov.**, and propose elevating *E. s. vicinus*, previously considered a subspecies of *Eozapus setchuanus*, to the status of an independent species. Furthermore, the uplift of the Qinghai-Tibetan Plateau, the complex topography of sky islands, and climate change promoted the speciation and diversity of the genus *Eozapus*.

Key Words

Eozapus, jumping mouse, new species, phylogenetic

Introduction

The mountains of southwestern China, which are known as "sky islands" (He and Jiang 2014), have been considered key biodiversity hotspots (Myers et al. 2000). The complex topography of the sky islands and diversified climate conditions may have led to the evolution of a unique fauna of endemic species and the emergence of new lineages (Wei et al. 2018). Previous phylogenetic and phylogeographic studies in this region have revealed cryptic new species of small mammals in the region, such as *Niviventer* (Zhang et al. 2016), *Crocidura* (Chen et al. 2020), the long-tailed mole (He et al. 2019), *Ochotona* (Koju et al. 2017), and Asian shrew-like moles (Wan et al. 2018).

The family Zapodidae is widespread, containing three genera, *Eozapus, Zapus,* and *Napaeozapus*, with only 11 species: *E. setchuanus, Z. hudsonius, Z. trtinotatus, Z. princeps, Z. luteus, Z. montanus, Z. oregonus, Z. pacificus, Z. saltator, N. abietorum, and N. insignis.* (Wilson and Mittermeier 2018; Mammal Diversity Database 2022). Fan et al. (2009) formerly presented molecular evidence confirming the validity of these three genera. Based on the discovery of an early Miocene fossilized tooth of the genus *Eozapus* in Inner Mongolia, researchers believe that this supports the hypothesis that Zapodidae originated in Asia (Smith and Xie 2008; Wilson and Mittermeier 2018).

Eozapus is one monotypic genus in Zapodidae, with an endemic species in the mountains of southwestern China and two subspecies, *Eozapus setchuanus setchuanus* (Pousargues, 1896) and *Eozapus setchuanus vicinus* (Thomas, 1912). However, there are differing opinions among researchers regarding the taxonomy of *Eozapus setchuanus*. Specifically, Fan et al. (2009) reported that the two subspecies of *Eozapus setchuanus* did not form reciprocally monophyletic taxa in the molecular phylogenetic tree,

Copyright *Yang, S. et al.* This is an open access article distributed under the terms of the Creative Commons Attribution License (CC BY 4.0), which permits unrestricted use, distribution, and reproduction in any medium, provided the original author and source are credited.

casting doubt on the traditional bifurcation of *E. setchuanus* into two subspecies. The other researchers agree with this taxonomic view (Cheng et al. 2021; Sui et al. 2022; Wei et al. 2022;). The molecular evolutionary history and the genetic differentiation of the two subspecies of this species have not yet been investigated in detail. Whether *E. s. vicinus* can be considered a separate and valid species has not yet been systematically analyzed from a molecular perspective (Michaux and Shenbrot 2017; Liu and Wu 2019; Cheng et al. 2021; Sui et al. 2022).

Due to the rarity of species within the genus *Eozapus*, capturing individuals is challenging. Consequently, the distribution of the two subspecies of *Eozapus setchuanus* remains poorly described in many regions. In this study, we collected 51 specimens of the genus *Eozapus* from southwestern China, which greatly improved the problem of under-sampling in previous studies (Fan et al. 2009). Morphological characteristics, principal component analysis of skulls, and mitochondrial and nuclear genes were analyzed to clarify the phylogenetic relationships within the genus *Eozapus*, determine the status of *E. s. vicinus* as a distinct species, and explore its evolutionary history.

Materials and methods

Sampling and DNA sequencing

In this study, 51 *Eozapus* specimens were collected from the Sichuan, Shaanxi, Gansu, and Ningxia provinces of China (Fig. 1, Table 1). Specimens were collected primarily using the snap trap method. Field surveys and collections of specimens both follow relevant laws and regulations in China. The field-collected samples were numbered, and morphological data (including body weight, tail length, ear height, and hindfoot length) were measured (Suppl. material 1: table S1). Liver and muscle tissues were obtained and preserved in analytically pure alcohol (99%). Upon return to the laboratory, tissues were stored in a -80 °C freezer for subsequent molecular analyses, while specimens were prepared as the study skins for morphological studies. All tissues and specimens used in this study were archived at the Sichuan Academy of Forestry (SAF) and the College of Life Sciences of Sichuan Normal University (SCNU) (Table 1).

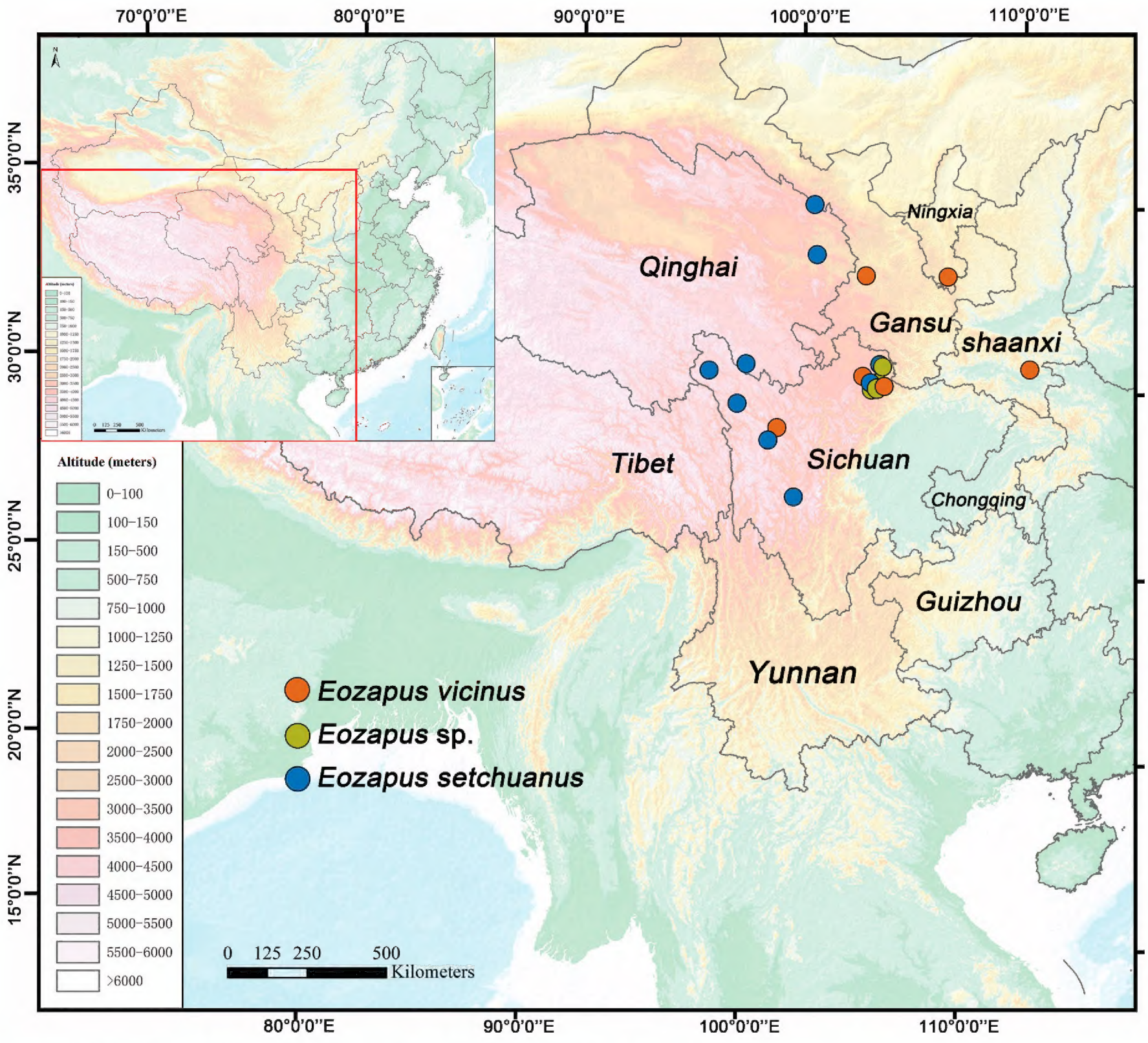

Figure 1. Map of the collection sites of the genus *Eozapus* in this study.

Table 1. Information on the collection sites of *Eozapus* specimens in this study (* represents topotype of *Eozapus* sp. and *E. setchuanus*).

Species	Field ID	Museum number	Genbank number			Locality	Longitude, Latitude	Elevation(m)
			CYT B	GHR	IRBP			
E. vicinus	csd2795	SAF13456	PQ723106	PQ752861	PQ752872	Hanzhong, Shaanxi, China	107.6301°E, 33.7101°N	2422
	csd2798	SAF11120	PQ723107	PQ752862	PQ752873	Guyuan, Ningxia, China	106.2746°E, 35.3905°N	2200
	csd2799	SAF11121	PQ723108	PQ752863	PQ752874	Guyuan, Ningxia, China	106.2746°E, 35.3905°N	2200
	csd2800	SAF11128	PQ723109	PQ752864	PQ752875	Guyuan, Ningxia, China	106.2936°E, 35.3781°N	2040
	csd2801	SAF11134	PQ723110	PQ752865	PQ752876	Guyuan, Ningxia, China	106.3279°E, 35.3676°N	2100
	csd2802	SAF11137	PQ723111	PQ752866	PQ752877	Guyuan, Ningxia, China	106.2746°E, 35.3905°N	2200
	csd2803	SAF11163	PQ723112	PQ752867	PQ752878	Guyuan, Ningxia, China	106.3279°E, 35.3676°N	2000
	csd2804	SAF11724	PQ723113	PQ752868	PQ752879	Songpan, Sichuan, China	103.562°E, 32.85°N	3110
	csd2965	SAF181316	PQ723114	PQ752869	PQ752880	Wanglang, Sichuan, China	104.0923°E, 32.9709°N	2600
	csd2967	SAF181367	PQ723115	-	-	Wanglang, Sichuan, China	104.7907°E, 32.0786°N	3000
	csd3532		PQ723116	-	-	Jiuzhaigou, Sichuan, China	103.9291°E, 33.0414°N	3037
	csd3576	SAF06319	PQ723117	PQ752870	PQ752881	Wanglang, Sichuan, China	104.0982°E, 32.9705°N	2614
	csd3577	SAF06352	PQ723118	-	-	Wanglang, Sichuan, China	104.7907°E, 32.0786°N	2614
	csd3581	SAF07345	PQ723119	PQ752871	PQ752882	Gannan, Gansu, China	103.5857°E, 34.9024°N	2780
Eozapus sp.	csd2808	SAF03225	PQ752960	-	-	Jiuzhaigou, Sichuan, China	103.8474°E, 33.0619°N	3100
	csd2814	*SAF181406	PQ752961	PQ752966	PQ752969	Wanglang, Sichuan, China	104.1571°E, 32.9526°N	\
	csd2970	*SAF191428	PQ752962	PQ752967	PQ752970	Wanglang, Sichuan, China	103.9919°E, 32.9308°N	3200
	csd2976	*SAF181458	PQ752963	PQ752968	PQ752971	Wanglang, Sichuan, China	103.9824°E, 32.9144°N	\
	csd2977	*SAF181457	PQ752964	-	-	Wanglang, Sichuan, China	103.9824°E, 32.9144°N	\
	csd5014	*SAF191248	PQ752965	-	-	Wanglang, Sichuan, China	104.0221°E, 32.0069°N	2931
E. setchuanus	csd1710	*SCNU03078	PQ752883	PQ752914	PQ752937	Kangding, Sichuan, China	101.5789°E, 29.788°N	3681
	csd1711	*SCNU03079	PQ752884	-	-	Kangding, Sichuan, China	101.5789°E, 29.788°N	3681
	csd1712	*SCNU03080	PQ752885	-	-	Kangding, Sichuan, China	101.5789°E, 29.788°N	3681
	csd2793	SAF13404	PQ752886	PQ752915	PQ752938	Guoluo, Qinghai, China	99.8186°E, 34.7792°N	3526
	csd2796	SAF12192	PQ752887	PQ752916	PQ752939	Shiqu, Sichuan, China	97.562°E, 32.854°N	3939
	csd2797	SAF12451	PQ752888	PQ752917	PQ752940	Haibei, Qinghai, China	99.8695°E, 38.2803°N	3150
	csd2806	SAF04507	PQ752889	PQ752918	PQ752941	Litang, Sichuan, China	99.8253°E, 29.5655°N	3450
	csd2962	SAF13391	PQ752890	-	-	Guoluo, Qinghai, China	100.5531°E, 33.4533°N	4152
	csd2973	SAF181425	PQ752891	PQ752919	PQ752942	Wanglang, Sichuan, China	104.0117°E, 32.9921°N	3526
	csd3532	SAF20721	PQ752892	-	-	Jiuzhaigou, Sichuan, China	103.9292°E, 33.0414°N	3037
	csd3545	*SAF11707	PQ752893	PQ752920	PQ752943	Kangding, Sichuan, China	101.831°E, 30.381°N	3870
	csd3547	*SAF11633	PQ752894	PQ752921	PQ752944	Kangding, Sichuan, China	101.84°E, 30.403°N	3490
	csd3548	*SAF11705	PQ752895	PQ752922	PQ752945	Kangding, Sichuan, China	101.831°E, 30.381°N	3870
	csd3549	*SAF11711	PQ752896	PQ752923	PQ752946	Kangding, Sichuan, China	101.831°E, 30.381°N	3870
	csd3550	*SAF11716	PQ752897	PQ752924	PQ752947	Kangding, Sichuan, China	101.831°E, 30.381°N	3870
	csd3551	*SAF11710	PQ752898	PQ752925	PQ752948	Kangding, Sichuan, China	101.831°E, 30.381°N	3870
	csd3552	*SAF11718	PQ752899	PQ752926	PQ752949	Kangding, Sichuan, China	101.831°E, 30.381°N	3870
	csd3553	*SAF11706	PQ752900	PQ752927	PQ752950	Kangding, Sichuan, China	101.832°E, 30.382°N	3871
	csd3554	*SAF11698	PQ752901	-	-	Kangding, Sichuan, China	101.84°E, 30.403°N	3840
	csd3555	*SAF11717	PQ752902	PQ752928	PQ752951	Kangding, Sichuan, China	101.831°E, 30.381°N	3870
	csd3556	*SAF11704	PQ752903	PQ752929	PQ752952	Kangding, Sichuan, China	101.831°E, 30.381°N	3871
	csd3557	*SAF12427	PQ752904	PQ752930	PQ752953	Kangding, Sichuan, China	99.594°E, 38.417°N	3275
	csd3558	*SAF11708	PQ752905	PQ752931	PQ752954	Kangding, Sichuan, China	99.8695°E, 38.2803°N	3870
	csd3559	*SAF11715	PQ752906	PQ752932	PQ752955	Kangding, Sichuan, China	101.831°E, 30.381°N	3870
	csd3560	*SAF11709	PQ752907	PQ752933	PQ752956	Kangding, Sichuan, China	101.831°E, 30.381°N	3870
	csd3579	SAF071043	PQ752908	PQ752934	PQ752957	Dege, Sichuan, China	104.0982°E, 32.9705°N	4145
	csd3583	SAF071076	PQ752909	-	-	Dege, Sichuan, China	103.9292°E, 33.0414°N	4150
	csd3584	SAF071021	PQ752910	-	-	Dege, Sichuan, China	107.6301°E, 33.7101°N	4010
	csd3585	SAF071080	PQ752911	PQ752935	PQ752959	Dege, Sichuan, China	106.2746°E, 35.3905°N	4010
	csd3587	SAF071063	PQ752912	PQ752936	PQ752958	Dege, Sichuan, China	99.1561°E, 31.8753°N	4020

The extraction of total DNA was carried out following the manufacturer's protocols for the animal liver or muscle tissue DNA extraction kit (Chengdu Fukuji Biological Co.). In this study, three genes were amplified for molecular phylogenetic and related analyses: one mitochondrial gene (CYT B, 1059 bp) and two nuclear genes (growth hormone receptor [GHR, 569 bp] and inverted repeat-binding protein [IRBP, 590 bp]). PCR amplifications were performed in a reaction volume mixture of 25 µl, containing 3 mM $MgCl_2$, 0.2 U rTaq polymerase (Takara, Dalian, China), 1 × reaction buffer, 0.2 mM of each dNTP, 0.4 mM of each primer, and approximately 100–500 ng of genomic DNA. The primers used for PCR amplification are listed in Suppl. material 1: table S1. PCR amplification was performed with an initial denaturation step at 94 °C for 5 min, followed by 35 cycles of denaturation at 94 °C for 45 s, annealing at 49–60 °C for 45 s, extension at 72 °C for 90 s, and a final extension step at 72 °C for 10 min. PCR products were identified using 1% agarose gel electrophoresis and then sent to QingKe Biological Co., Ltd. for purification and bidirectional Sanger sequencing.

Sequencing results were aligned preliminarily using MEGA v5 (Tamura et al. 2013). All sequences were manual corrections edited to ensure the proper translation, thereby avoiding potential impacts on subsequent analyses. CYT B, IRBP, and GHR sequences from the selected *Eozapus* species and the outgroup *Stylodipus sungorus*, *Stylodipus andrewsi,* and *Stylodipus telum* were downloaded from GenBank (Suppl. material 1: table S2).

Phylogenetic analyses

Three datasets were created for phylogenetic analysis: 1) a mitochondrial dataset (CYT B), 2) a nuclear gene dataset (nuDNA), and 3) an all-gene combined dataset (CYT B + nuDNA). The optimal base substitution model for each dataset was determined using jModelTest 2.1.7 (Posada 2008), and the Akaike information criterion (AIC) was used to assess the fitness of each model (Luo et al. 2010). The optimal substitution models for each gene and dataset are listed in Suppl. material 1: table S3.

Phylogenetic trees were constructed using Bayesian inference (BI) based on the three established datasets. The MrBayes 3 program was used to reconstruct the BI tree (Ronquist and Huelsenbeck 2003). Parameter settings for the BI tree were based on those described by Chen et al. (2012). Posterior distributions were obtained using the Markov chain Monte Carlo (MCMC) method with one cold chain and three heated chains for 100 million generations at a sampling interval of 10,000. The first 2,000 generations were treated as burn-ins. The Markov chain MCMC runs were repeated twice to confirm a consistent approximation of the posterior parameter distributions. Figtree v1.4.3 was used to visualize the BI tree output, and a posterior probability (PP) > 0.95 was considered strong support (Huelsenbeck and Rannala 2004).

Genetic distance and species delimitation

Genetic distances between clades were calculated based on the CYT B gene using the Kimura 2-parameter model in MEGA v5.05 (Tamura et al. 2011).

BPP v3.0 was used to test the hypothesis of independent evolutionary lineages represented by populations (Yang and Rannala 2010; Yang et al. 2012; Yu et al. 2013). To verify the genetic differentiation detected in the genus *Eozapus*, the gene tree constructed in the previous step was used as a guide tree, and the validity of our assignment of the three putative species was tested in BPP v3.1. The analysis of Chen et al. (2022) was followed, which was defined using Algorithm 0 and Algorithm 1, with τ representing the root age of the species tree and θ representing the size parameter of the population. These two important parameters significantly affect the posterior probability of the BPP (Yang and Rannala 2010; Pan et al. 2019; Chen et al. 2022). Twelve analyses were conducted using three different prior combinations of τ and θ: (1) τ = G (2, 2000), θ = G (2, 2000); (2) τ = G (1, 10), θ = G (2, 2000); and (3) τ = G (1, 10), θ = G (1, 10) (Leaché and Fujita 2010). Each rjMCMC was run for 100,000 generations, with samples collected every 100 generations after discarding 10,000 generations as preburn-in. When the posterior probability exceeded 0.95, the analysis supports that each evolutionary branch is a separate species.

Divergence time

Since mitochondrial genes may lead to an earlier estimated differentiation time (Phillips 2009; Zheng et al. 2011), the nuclear gene dataset was used for estimation in this study. The time of differentiation of the genus *Eozapus* was analyzed and imputed using BEAST v1.7.5 (Drummond et al. 2012) based on the nuDNA dataset. Four fossil calibration points were used in this study, as described by Shenbrot et al. (2017). (1) *Stylodipus* and *Chimaerodipus* originated within the Dipodinae at approximately 3.84–5.49 Ma (mean = 4.85, standard deviation = 0.61, upper 95% = 3.84–5.85 Ma). (2) *Eremodipus* and *Jaculus* originated within the Dipodidae at approximately 3.75–5.74 Ma (mean = 4.73, standard deviation = 0.61, upper 95% = 3.73–5.73 Ma). (3) Differentiation of *Jaculus* occurs at approximately 1.18–2.31 Ma (mean = 1.73, standard deviation = 0.354, upper 95% = 1.15–2.31 Ma). (4) Dipodinae originated at approximately 9.46–11.47 Ma (mean = 10.53, standard deviation = 0.65, upper 95% = 9.46–11.60 Ma). The remaining parameters were set as described by Chen et al. (2022).

Morphological data and analyses

A total of 17 complete skull specimens of intact adult individuals were obtained and measured using digital Vernier calipers, with an accuracy of 0.01 mm, as described previously (Liu et al. 2007, 2012; Patton and Conroy 2017). The measurement metrics included body weight (BW), head-body length (HBL), tail length (TL), hind-foot length (HFL), ear length (EL), profile length (PL), skull basal length (SBL), median palatal length (MPL), zygomatic breadth (ZB), least breadth between the orbits (LBO), brainstem breadth (BB), height of the braincase (HB), auditory bulla length (ABL), upper toothrow length (UTRL), length of the upper molars (LUM), upper molar row breadth (UMRB), mandibular length (ML), lower toothrow length (LTRL), and length of the lower molar row (LLMR). Because external measurement data may display differences between different measurers, they were not used for the morphological analysis. SPSS v17.0 was used to analyze the measurement values of the indicators. When the data satisfied a normal distribution, principal component analysis (PCA) was used to evaluate the overall similarity between species, and discriminant analysis (DA) was used to determine whether the classification was correct.

Results

Phylogenetic analyses

We obtained 51 CYT B sequences of 1059 bp and 37 nuclear gene sequences of 1159 bp (GHR: 569 bp; IRBP: 590 bp). The new sequences were deposited in GenBank (Accession Numbers PQ723106–PQ723119, PQ75286–PQ752971, Table 1). MrBayes was used to reconstruct phylogenetic relationships based on the three datasets, and all three topological structures obtained were largely consistent (Fig. 2). BI results based on three different datasets supported the division of the genus *Eozapus* into three clades. *E. vicinus* was monophyletic and was consistently positioned as the most basal lineage across all three datasets (CYT B: PP = 1.00, nuDNA = 0.38, and CYT B + nuDNA = 1.00). *Eozapus* sp. was identified as a sister group of *E. setchuanus*. In the CYT B phylogenetic tree, evolutionary relationships within this taxon were highly supported. The CYT B + nuDNA gene tree was identical and well supported (PP = 1.00) by the topology of this taxon in the CYT B gene tree (Fig. 2).

Genetic distances and species delimitation

The K2P genetic distances between the three clades of *Eozapus* based on the CYT B gene are shown in Table 2. The results revealed that the genetic distance values ranged from 10.9% to 17.8%. The genetic distance value between *E. vicinus* and *Eozapus* sp. was at 17.8%, followed by 16.6% between *E. vicinus* and *E. setchuanus*, and 10.9% between *Eozapus* sp. and *E. setchuanus* was the smallest. Genetic distances among all species showed good species-level variation.

Table 2. Kimura two-parameters (K2P) genetic distances in the genus *Eozapus* based on the CYT B gene.

	E. vicinus	***Eozapus* sp.**
E. vicinus		
Eozapus sp.	0.178	
E. setchuanus	0.166	0.109

The results from BPP based on the CYT B + nuDNA and nuDNA datasets produced 36 results, all of which strongly supported the division of *Eozapus* into three clades (PP = 1.00; Suppl. material 1: table S4).

Molecular divergence estimation

The results indicated that the most recent common ancestor of *Eozapus* dates back to the Miocene (8.15 Ma, 95% CI = 5.23–10.62), marking the divergence of *E. vicinus* from the other two species. The divergence time of *Eozapus* sp. and *E. setchuanus* (6.12 Ma, 95% CI = 3.41–9.16) occurs in the Miocene (Fig. 3).

Morphological analysis

A total of 14 craniodental and 5 external indicators were measured (Suppl. material 1: table S5). External indicators were excluded from the morphological analysis because of potential interobserver variation in measurements (Jiang et al. 2003). Additionally, owing to damage to the zygomatic bones of several specimens during handling, ZB measurements were excluded from the analysis, leaving 13 skull measurements for morphological analysis (Table 3).

The results of the PCA based on 13 cranial measurements revealed that the two principal components explained

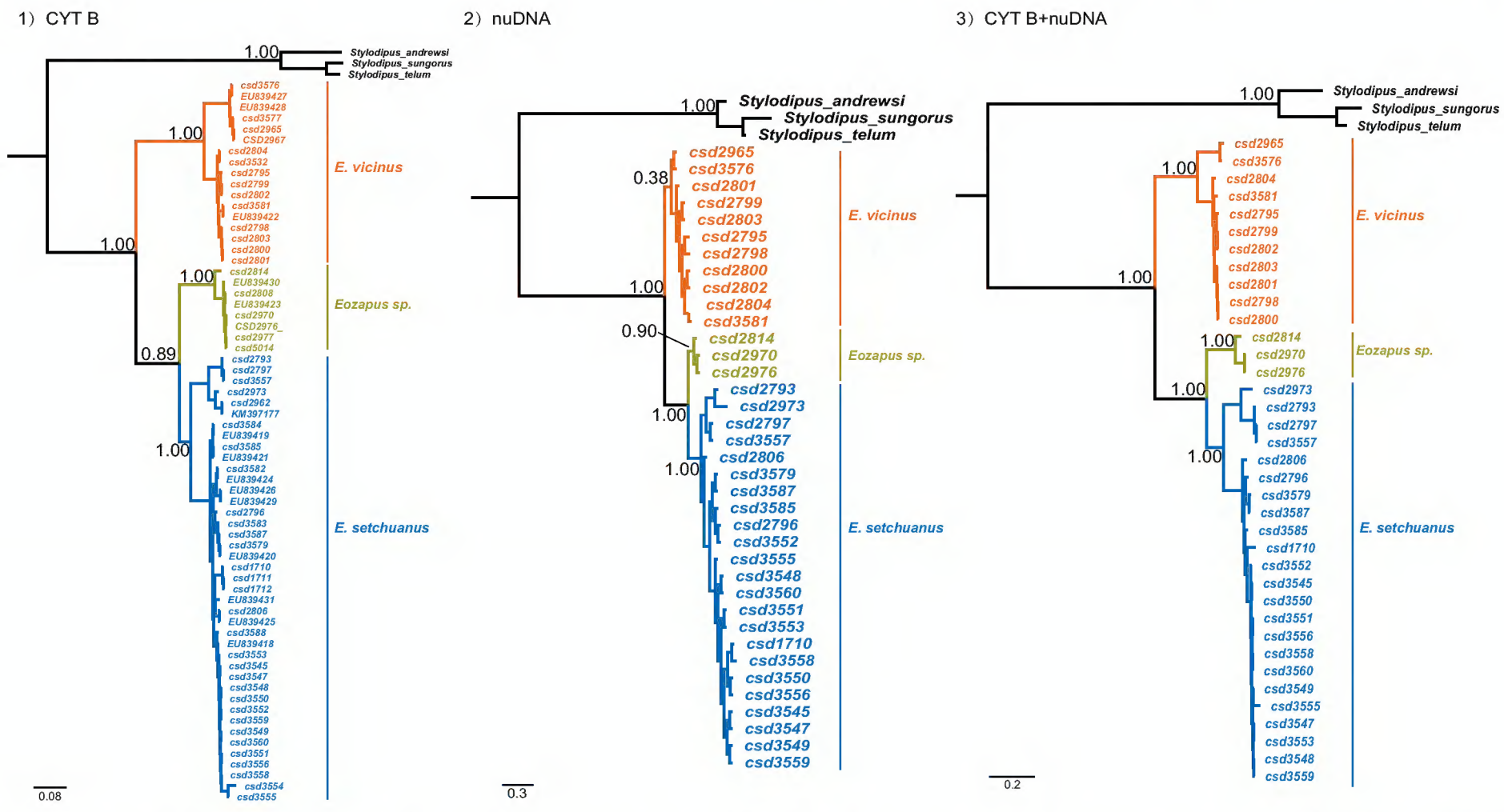

Figure 2. Bayesian phylogenetic analyses based on the CYT B dataset, the nuDNA dataset, and the CYT B+nuDNA dataset. The numbers above the branches refer to Bayesian posterior probabilities (PP).

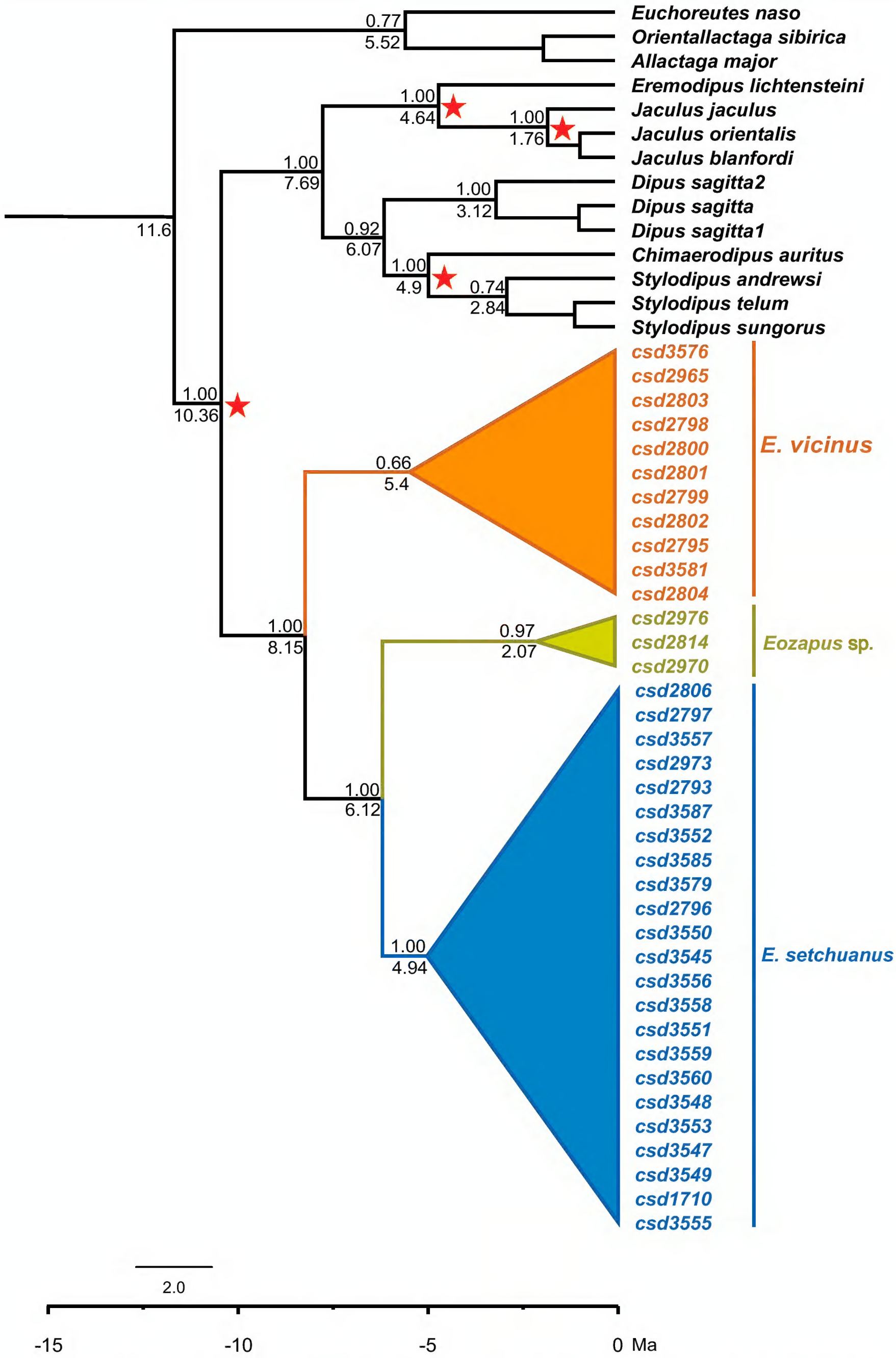

Figure 3. Divergence times estimated using BEAST based on the nuDNA dataset. Branch lengths represent time. Numbers above the nodes indicate posterior probabilities (PP). Numbers below the nodes represent the median divergence time. The four asterisks indicate fossil-calibrated nodes.

Table 3. The average and standard deviation of the measurement data of the skull morphology of the specimens of the genus *Eozapus* used in this study.

Measurements	*E. vicinus* n = 7	*Eozapus* sp. n = 3	*E. setchuanus* n = 7
PL	22.12 ± 1.06	21.58 ± 0.67	22.16 ± 1.15
	20.37–24.09	20.83–22.12	20.20–23.73
SBL	16.58 ± 1.12	16.22 ± 0.65	16.87 ± 0.89
	14.25–18.10	15.50–16.77	15.75–18.22
MPL	9.77 ± 0.52	9.62 ± 0.41	9.96 ± 0.47
	8.69–10.48	9.17–9.97	9.12–10.48
LBO	3.94 ± 0.13	3.76 ± 0.20	3.95 ± 0.17
	3.69–4.15	3.63–3.99	3.79–4.30
BB	10.16 ± 0.44	10.24 ± 0.27	10.51 ± 0.40
	9.20–10.71	9.98–10.52	9.72–10.96
HB	8.19 ± 0.11	8.11 ± 0.14	8.42 ± 0.48
	8.03–8.40	8.02–8.27	7.86–9.38
ABL	5.81 ± 0.11	5.84 ± 0.12	6.05 ± 0.22
	5.56–5.95	5.71–5.92	5.88–6.52
UTRL	9.83 ± 0.57	9.51 ± 0.12	10.26 ± 0.48
	8.54–10.44	9.37–9.61	9.35–10.89
LUM	3.72 ± 0.29	3.87 ± 0.14	4.02 ± 0.08
	3.00–3.92	3.71–3.98	3.95–4.14
UMRB	4.87 ± 0.11	4.80 ± 0.10	5.01 ± 0.11
	4.70–5.03	4.74–4.91	4.78–5.11
ML	13.01 ± 0.63	12.49 ± 0.23	13.21 ± 0.70
	11.82–14.07	12.24–12.69	12.12–14.05
LTRL	8.46 ± 0.51	8.01 ± 0.06	8.65 ± 0.46
	7.28–9.07	7.96–8.07	8.08–9.31
LLMR	3.47 ± 0.39	3.62 ± 0.05	3.86 ± 0.10
	2.51–3.65	3.57–3.66	3.75–4.03

Notes: PL: profile length; SBL: skull basal length; MPL: median palatal length; LBO: least breadth between the orbits; BB: braincase breadth; HB: height of the braincase; ABL: auditory bulla length; UTRL: upper toothrow length; LUM: length of upper molars; UMRB: upper molar row breadth; ML: mandibular length; LTRL: lower toothrow length; LLMR: length of lower molar row.

77.049% of the variance (Table 4). The first principal component (PC1) accounted for 59.533% of the variance and showed positive factor loadings. PL, SBL, and MPL had factor loadings > 0.9, indicating a strong correlation with PC1, Factor loadings > 0.8 included UTR, ML, and LTRL. The second principal component (PC2) explained 17.516% of the variance and had mostly negative factor loadings, with LUM and LLMR being the largest loading, correlating strongly with PC2. It also was negatively correlated with LBO (loadings < - 0.2) (Table 4). The PCA results indicated that most individuals were effectively classified into three species with minimal overlap (Fig. 4).

Table 4. Percent variance explained on the two components of PCA of cranial measurements of *Eozapus*.

Variables	PC1	PC2
PL	0.949	0.049
SBL	0.924	0.163
MPL	0.930	0.124
LBO	0.514	-0.236
BB	0.597	0.168
BH	0.629	0.578
ABL	0.250	0.878
UTR	0.835	0.459
LUM	0.088	0.945
UMR	0.786	0.402
ML	0.839	0.343
LTRL	0.810	0.378
LLMR	0.111	0.929
Eigenvalue	7.739	2.277
Explained(%)	59.533	17.516

Discriminant analysis (DA) showed that the three specimens within *Eozapus* were accurately classified (Fig. 4). Correct taxonomic determination was obtained for 100.0% of the original grouped samples, and cross-validation results indicated that 100% of the samples were correctly classified.

The skull of *Eozapus* sp. is the smallest (average PL = 21.58 mm), while that of *E. setchuanus* is 22.16 mm and *E. vicinus* is 22.37 mm. In fact, the average skull measurement of *Eozapus* sp. was less than that of the other two species. The SBL (average = 16.22 mm), UTRL (average = 9.51 mm), ML (average = 12.49 mm), and LTRL (average = 8.01 mm) of *Eozapus* sp. were the shortest, whereas the UTRL (average = 10.26 mm), ML (average = 13.21 mm), and LTRL (average = 8.65 mm) of *E. setchuanus* are the longest (Table 3). The tooth formula of this genus is 1.0.1.3/1.0.0.3. Depression of the occlusal surface of the upper molars in the genus *Eozapus* is variable; *E. vicinus* is slightly concave, *Eozapus* sp. is moderate, while *E. setchuanus* is severely concave (Fig. 5a2, b2, c2, a6, b6, c6). The lengths of the first and second lower molars are nearly equal, and the third lower molar (m_3)

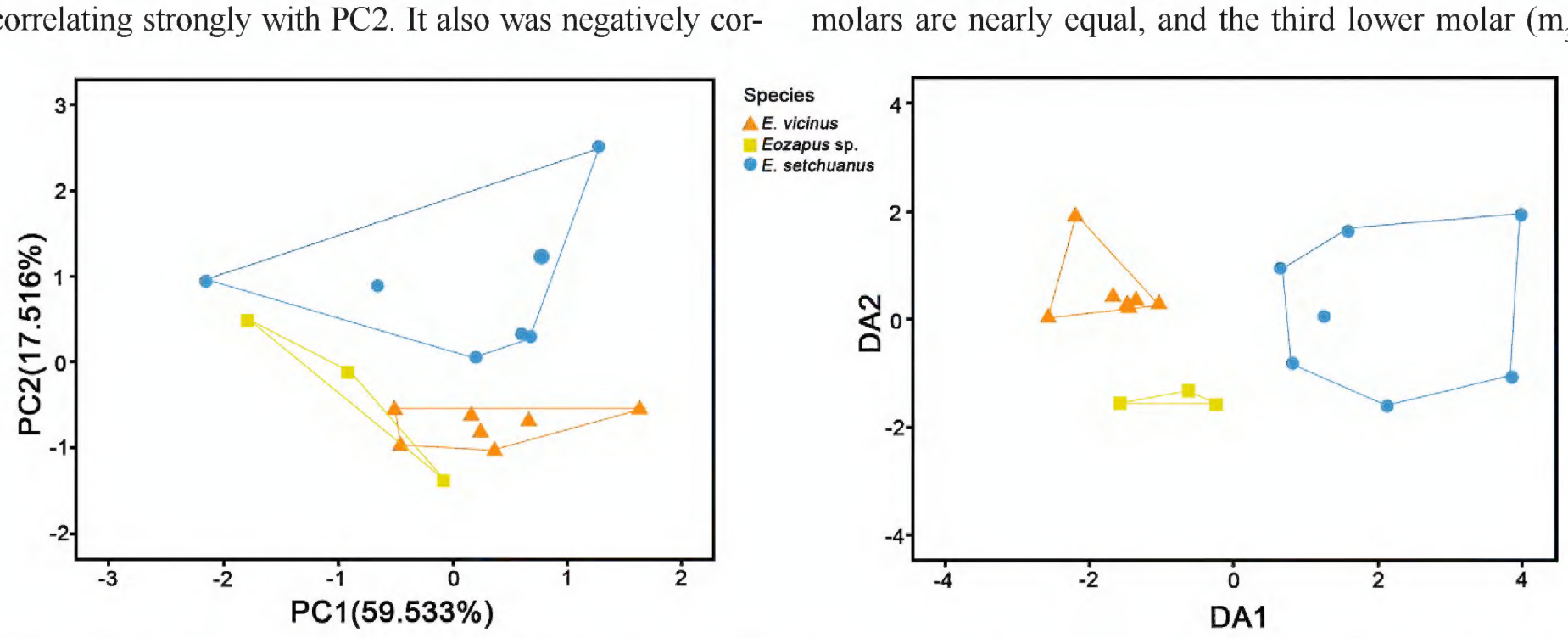

Figure 4. Result of the principal component analysis (PCA) and the discriminant analysis (DA) based on skull measurement data of the genus *Eozapus*.

is reduced (approximately 30%). On the second lower molar (m_2), the metalophid of *E. vicinus* penetrated the entire surface of the second lower molar (m_2) from the middle, whereas for *Eozapus* sp. and *E. setchuanus*, the metalophid of the m_2 is discontinuous and concave inward medially (Fig. 5a6, b6, c6). In addition, *Eozapus* sp. has a distinctly depressed longitudinal groove in the middle of the third lower molar (m_3) and towards the lingual side (Fig. 5b6); the m_3 of *E. vicinus* is flat in the middle (Fig. 5a6), and *E. setchuanus* also has a depressed longitudinal groove in the middle of the third lower molar (m_3), but differs from *E. vicinus* in that it is directed to the buccal side (Fig. 5c6).

Hair characteristics of the genus *Eozapus* are as follows (Fig. 6d). The color of the dorsal and notal hairs was the same in all three species, brownish yellow, but *E. vicinus* was slightly lighter than *Eozapus* sp., while in *E. setchuanus* the extent of the yellow wash on the individual hairs extended further towards the root (Fig. 6). (1) *E. vicinus* exhibits pure white at the base and tip of hair in its abdomen. (2) *Eozapus* sp. has no brownish-yellow longitudinal stripes on its chest, and its hair base is white with yellow tips on its abdomen. (3) *E. setchuanus* has a brownish-yellow longitudinal stripe on its chest. The hair at the base was purely white with yellowish tips on its abdomen.

Based on the distinct morphological characteristics and deep genetic divergence described in the preceding sections, we recognized the jumping mouse from the Wanglang National Nature Reserve as a distinct, undescribed species within *Eozapus* and formally described it as follows.

Eozapus wanglangensis Yang, Liu & Chen, sp. nov.

https://zoobank.org/B9AA3CF7-0465-4415-B65E-0BC65D58C665

Suggested common name in English: Wanglang jumping mouse

Suggested common name in Chinese: 王朗林跳鼠 [Wang Lang Lin Tiao Shu]

Type material. ***Holotypes*:** • An adult female (SAF191248) captured by Rui Liao and Xuming Wang in September 2019 from the Wanglang National Nature Reserve, Pingwu, Sichuan Province, China (32.0069°N, 104.0221°E; 2931 m a.s.l.). The study skin and skull specimens have been deposited at the Sichuan Academy of Forestry (SAF).

Paratypes (n = 5): • Three specimens (SAF181406♂, SAF181457♀, and SAF181458♀) were collected by Rui Liao, Xuming Wang, and Haijun Jiang in September 2018 from the type locality at elevations ranging from 2900 to 3200 m. • One specimen of unknown sex (SAF06364) was collected by Shaoying Liu in 2006 from the type locality. • One female specimen (SAF03225♀) was collected by Zhiyu Sun in June 2003 from Jiuzhaigou, Sichuan Province, China (33.0619°N, 103.8474°E; 3100 ma. s.l.).

Measurements of holotype (mm). BW = 27 g; HBL = 78.00; TL = 120.00; HFL = 28.00; EL = 13.00; PL = 21.78; SBL = 16.39; MPL = 9.97; LBO = 3.66; BB = 9.98; HB = 8.02; ABL = 5.90; UTRL = 9.61; LUM = 3.91; UMRB = 4.74; ML = 12.96; LTRL = 8.07; LLMR = 3.64; ZB = 10.09.

Etymology. The special name "Wanglang" refers to the Wanglang National Nature Reserve, the type locality of the new species, known for its rich biodiversity. We suggest "Wanglang jumping mouse" as the English common name and "王朗林跳鼠 (Wang lang Lin tiao shu)" as the Chinese common name.

Diagnosis. Slender body, longer hindfoot, adapted for jumping. The head-body length (HBL) averages approximately half as long as the total length (TL) and is slightly shorter or longer than half the TL. The skull is smaller than that of the other two species of *Eozapus*. Physical characteristics include a brownish-yellow body on the back. The tail is slender and covered with sparse, short, tan hairs, and the scales are conspicuous. It is distinguished from other species based on the following features: (1) Abdominal hair coloration differs from that of the other two species of *Eozapus*. Compared to the pure white abdominal hairs of *E. vicinus*, the abdominal hairs of this species are white at the base and yellow at the tips. *E. setchuanus* has a brownish-yellow longitudinal stripe on the abdomen, which is absent in this species.; (2) The second lower molar (m_2) has a longitudinal deep groove, and the metalopaid is concave inward medially; (3) a distinctly depressed longitudinal groove in the middle of the third lower molar (m_3) and towards the lingual side

Description. Small jumping mouse with a head-body length of 65–78 mm (average 71 mm) and tail length of 120–132 mm (average 126 mm), featuring a distinctly bicolored (grayish to brown) tail above and white below (HBL/TL = 0.56). Hind foot length ranges from 28 to 30 mm (average 29 mm), with ear height measuring 12–15 mm (average 13 mm). The muzzle was light brown with a tan ring above the nasal pads. The dorsum of the body is bright rusty brown with a longitudinal brown stripe from the forehead through the eyes to below the eyes and between the ears and the base of the tail. Abdominal hair has a white base and a light-yellow tip, clearly distinguishing the coloration between the back and abdomen. The tail was slender and covered with sparse, short, yellowish-brown hairs. All four feet are beige, with shorter forefeet and elongated hind limbs and hind feet.

The skull of *E. wanglangensis* sp. nov. is the smallest in the genus *Eozapus*, measuring 21.58 ± 0.67 mm. It features a curved cranial surface with the highest point at the junction of the frontal and parietal bones. The muzzle is slender, with the anterior end of the nasal bone much longer than the anterior end of the maxillary incisors. The skull has a well-developed and pronounced sagittal crest, a wider interorbital region, slender and curved zygomatic bones, nearly parallel zygomatic arches on both sides, and small auditory bullae. Compared to other *Eozapus* species, the skull length (SBL) of *E. wanglangensis* sp. nov. is the smallest, averaging 16.22 mm.

The maxillary incisors of *E. wanglangensis* sp. nov. are orange-red and vertically oriented, with pronounced longitudinal grooves on their anterior margins. The premolars are small and round. The first upper molar (M^1) is larger than the second, featuring four small, equal cusps on its occlusal surface with deep concave folds on both the buccal and lingual sides. The third upper molars (M^3)

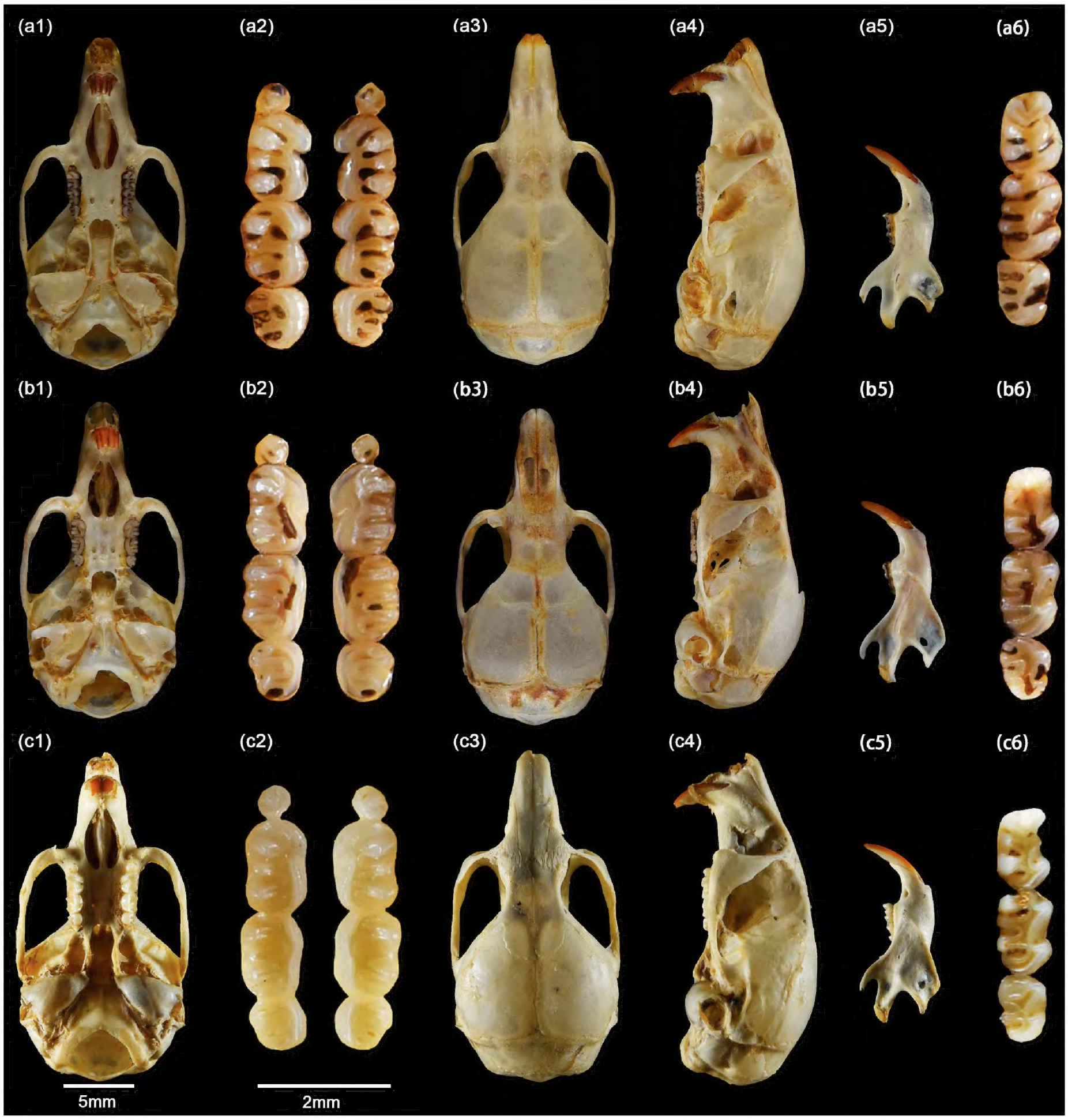

Figure 5. Skulls and tooth comparison among species of the genus *Eozapus*. **a.** *E. vicinus* **a1–a6**; **b.** *Eozapus* sp. **b1–b6**; **c.** *E. setchuanus* c1-c6 holotype; (1) ventral view; (2) upper tooth row; (3) dorsal view; (4) lateral view; (5) lower jaws; (6) lower tooth row; The red arrow indicates the position of the dental variation.

are the smallest. The anterior third of the anterior margin of the first upper molar (M^1) exhibits a concave fold that divides the tooth into an anterior inner lobe, with five prominent small transverse lobes on the outer side. The second and fourth lobes are taller than the other lobes. However, the second upper molar (M^2) lacks an anterior inner lobe (Fig. 5b2). The lower molars all have four distinct medial lobe-like projections. The first lower molar (m_1) is almost the same size as the second lower molar (m_2), with one concave fold on the anterior margin and two folds on the lateral side. The second and third lower molars each have one medial concave fold. There is a distinctly depressed longitudinal groove in the middle of the third lower molar (m_3) (Fig. 5b6).

Distribution and ecology. *E. wanglangensis* sp. nov. is primarily found in the Wanglang National Nature Reserve and central Jiuzhaigou County, Sichuan Province. This species inhabits forests and forest-edge grasslands at altitudes ranging from 1800 to 3100m, preferring forests with denser shrubs and streams.

Comparisons. *E. wanglangensis* sp. nov. is the smallest species of *Eozapus*, with a head-body length-to-total length ratio (HBL/TL) of 0.56. In comparison, *E. setchuanus* has an HBL/TL ratio of 0.65, whereas *E. vicinus* has an HBL/TL ratio of 0.61. Compared to *E. setchuanus* (UTRL = 10.26 ± 0.48 mm; UMRB = 5.01 ± 0.11 mm) and *E. vicinus* (UTRL = 9.83 ± 0.57 mm; UMRB = 4.87 ± 0.11 mm), *E. wanglangensis* sp. nov. exhibits smaller values for

Figure 6. Pelage comparisons among species of the genus *Eozapus*: **a.** *Eozapus vicinus* (museum number SAF11163); **b.** *Eozapus* sp. (museum number SAF191248); **c.** *Eozapus setchuanus* (museum number SAF11706); **d.** Hair variation (below chest to hindfoot); (1) dorsal view; (2) ventral view; (3) lateral view.

UTRL (9.51 ± 0.12 mm) and UMRB (4.80 ± 0.10 mm). *Eozapus wanglangensis* sp. nov. has no brownish-yellow longitudinal stripes on its chest, and its hair base is white with yellow tips on its abdomen. This species differs in that the second lower molar (m_2) is discontinuous on the mesofossette and has a longitudinal groove medially, and there is a distinctly depressed longitudinal groove in the middle of the third lower molar (m_3) and towards the lingual side.

Discussion

Geological formations and climate change have been closely linked to the evolution of small mammals (Li et al. 2022). The complex topography and geographic history of the "sky islands," along with diversified climate conditions, may have led to the evolution of the endemic *Eozapus* species and the emergence of new species. Our study reveals that the origin of species within the genus *Eozapus* dates to the Miocene. We hypothesize that climate change during the Miocene facilitated the expansion and divergence of *Eozapus* species. The speciation and evolution of this genus were closely associated with the uplift of the Qinghai-Tibetan Plateau (QTP). Previous studies have suggested that the QTP uplifted several times, one of which was 6–8 Ma ago (Molnar et al. 1993; Molnar 2005; Song et al. 2007). This geological movement has altered the climate and topographic structure of the region, creating isolation between mountain ranges and promoting the allopatric speciation, dispersal, and divergence of species, thereby providing a foundation for biodiversity. The divergence times observed within the genus *Eozapus* closely coincided with the uplift time of the QTP.

It is worth noting that the species within *Eozapus* are quite genetically distinct and have been isolated/separate for a long evolutionary time but appear similar from external morphology. It is possible that each mountain in the 'sky islands' has acted as refugia and provided the only continuously suitable habitats for *Eozapus* since the Miocene. After long-term isolation, populations in each refugium likely became isolated in situ, resulting in allopatric speciation. Previous phylogenetic and phylogeographic investigations have revealed cryptic species of small mammals in this "sky islands" region (Koju et al. 2017; Wan et al. 2018; He et al. 2019; Chen et al. 2020).

A previous study by Fan et al. (2009) revealed that *Eozapus setchuanus* and *E. vicinus*, previously considered as two subspecies of *E. setchuanus*, did not form reciprocally monophyletic lineages. We hypothesize that this conclusion may be attributed to several factors, including the single origin of the samples, the limited sample size, and the authors' morphological judgment based primarily on geographic distribution. Notably, the three *Eozapus* species are known to be distributed in the Wanglang Nature Reserve of Sichuan Province (Table 1). In this study, we addressed these issues and established the independence of the three species of the genus *Eozapus* from comprehensive molecular and morphological analyses.

Conclusion

In this study, we reorganized the phylogenetic relationships of the genus *Eozapus* through molecular and morphological analyses and reassessed the species diversity of this genus. These results indicated that the *Eozapus* species are quite genetically distinct and have a long evolutionary history in the sky islands of southwestern China, but they appear quite similar in convergent external morphology. We describe a new species, *Eozapus wanglangensis* sp. nov., and suggest elevating *E. s. vicinus*, previously considered a subspecies of *E. setchuanus*, as a distinct species, *E. vicinus*. Furthermore, the uplift of the Qinghai-Tibetan Plateau, the complex topography of sky islands, and climate change promoted the speciation and diversity of the genus *Eozapus*.

Acknowledgments

The study is supported by the National Natural Science Foundation of China (32070424) to Shunde Chen; the National Natural Science Foundation of China (32370496) to Shaoying Liu; the Natural Science Foundation of Sichuan Province (25NSFSC0983) to Shunde Chen; and the Experimental Technology Project of Sichuan Normal University (SYJS2023018).

References

Chen SD, Qing J, Liu Z, Liu Y, Tang MK, Murphy RW, Pu YT, Wang XM, Tang KY, Guo KJ, Jiang XL, Liu SY (2020) Multilocus phylogeny and cryptic diversity of white-toothed shrews (Mammalia, Eulipotyphla, *Crocidura*) in China. BMC Evolutionary Biology 20: 29. https://doi.org/10.1186/s12862-020-1588-8

Chen SD, Tang KY, Wang XM, Li FJ, Fu CK, Liu Y, Abu ul Hassan Faiz, Jiang XL, Liu SY (2022) Multi-locus phylogeny and species delimitations of the striped-back shrew group (Eulipotyphla, Soricidae): Implications for cryptic diversity, taxonomy and multiple speciation patterns. Molecular phylogenetics and evolution 177: 107619. https://doi.org/10.1016/j.ympev.2022.107619

Cheng JL, Xia L, Wen ZX, Zhang Q, Ge DY, Yang QS (2021) Review on the systematic taxonomy of Dipodoidea in China. Acta Theriologica Sinica 41(3): 275–283. https://doi.org/10.16829/j.slxb.150531

Drummond AJ, Suchard MA, Xie D, Rambaut A (2012) Bayesian phylogenetics with BEAUti and the BEAST 1.7. Molecular biology and evolution 29(8): 1969–1973. https://doi.org/10.1093/molbev/mss075

Fan ZX, Liu SY, Liu Y, Zeng B Guo C, Yue B (2009) Molecular phylogeny and taxonomic reconsideration of the subfamily Zapodinae (Rodentia, Dipodidae), with an emphasis on Chinese species. Molecular Phylogenetics and Evolution 51(3): 447–453. https://doi.org/10.1016/j.ympev.2009.03.005

He K, Eliécer E, Gutiérrez, Heming NM, Koepfli K, Wan T, He S, Jin W, Liu SY, Jiang XL (2019) Cryptic phylogeographic history sheds light on the generation of species diversity in sky-island mountains. Journal of Biogeography 46: 2232–2247. https://doi.org/10.1111/jbi.13664

He K, Jiang XL (2014) Sky islands of southwest China. I: An overview of phylogeographic patterns. Chinese Science Bulletin 59: 585–597. https://doi.org/10.1007/s11434-013-0089-1

Huelsenbeck J, Rannala B (2004) Frequentist properties of Bayesian posterior probabilities of phylogenetic trees under simple and complex substitution models. Systematic biology 53(6): 904–913. https://doi.org/10.1080/10635150490522629

Jiang XL, Wang YX, Hoffmann RS (2003) A review of the systematics and distribution of Asiatic short-tailed shrews, genus Blarinella (Mammalia, Soricidae). Mammalian Biology 68(4): 193–204. https://doi.org/10.1078/1616-5047-00085

Koju NP, He K, Chalise MK, Ray C, Chen ZZ, Zhang B, Jiang XL (2017) Multilocus approaches reveal underestimated species diversity and inter-specific gene flow in pikas (Ochotona) from southwest-ernChina. Molecular Phylogenetics and Evolution 107: 239–245. https://doi.org/10.1016/j.ympev.2016.11.005

Leaché AD, Fujita MK (2010) Bayesian species delimitation in West African forest geckos (Hemidactylus fasciatus). Proceedings. Biological sciences 277(1697): 3071–3077. https://doi.org/10.1098/rspb.2010.0662

Li Q, Li Q, Xu RC, Wang YQ (2022) Rodent faunas, their paleogeographic pattern, and responses to climate changes from the early Eocene to the early Oligocene in Asia. Frontiers in Ecology and Evolution 10: 955779. https://doi.org/10.3389/fevo.2022.955779

Liu SY, Wu Y (2019) Handbook of the mammals of China. Strait Book Company.

Liu SY, Sun ZY, Zeng ZY, Zhao EM (2007) A new species (*Proedomys*: Aricolinae: Murida) from the Liangshan Mountains of Sichuan Province, China. Journal of Mammalogy 5: 1170–1178. https://doi.org/10.1644/06-MAMM-A-141R2.1

Liu SY, Liu Y, Guo P, Sun ZY, Murphy RW, Fan ZX, Fu JR, Zhang YP (2012) Phylogeny of oriental voles (Rodentia, Muridae, Arvicolinae): Molecular and morphological evidence. Zoological Science 9: 610–622. https://doi.org/10.2108/zsj.29.610

Luo A, Qiao H, Zhang Y, Shi W, Ho SY, Xu W, Zhang A, Zhu C (2010) Performance of criteria for selecting evolutionary models in phylogenetics: a comprehensive study based on simulated datasets. BMC evolutionary biology 10: 242. https://doi.org/10.1186/1471-2148-10-242

Mammal Diversity Database (2022) Mammal Diversity Database (Version 1.9.1). Zenodo. https://doi.org/10.5281/zenodo.4139818

Michaux J, Shenbrot G (2017) Family Dipodidae (Jerboas). Handbook of the mammals of the world, 7. Rodents II. Barselonain: Lynx Edicionsin in association with Conservation International and IUCN.

Molnar P (2005) Mio-pliocene growth of the Tibetan Plateau and evolution of East Asian climate. Palaeontologia Electronica 8(2A): 23P.

Molnar P, England P, Martinod J, (1993) Mantle Dynamics, Uplift of the Tibetan Plateau, and the Indian Monsoon. Reviews of Geophysics 31: 357–396. https://doi.org/10.1029/93RG02030

Myers N, Mittermeier RA, Mittermeier CG, Fonseca GABD, Kent J (2000) Biodiversity hotspots for conservation priorities. Nature 403: 853–858. https://doi.org/10.1038/35002501

Pan T, Sun Z, Lai XL, Orozcoterwengel P, Yan P, Wu G, Wang H, Zhu W, Wu X-B, Zhang B-W (2019) Hidden species diversity in Pachyhynobius: A multiple approaches species delimitation with mitogenomes. Molecular phylogenetics and evolution 137: 138–145. https://doi.org/10.1016/j.ympev.2019.05.005

Patton JL, Conroy CJ (2017) The conundrum of subspecies: Morphological diversity among desert populations of the California vole (Microtus californicus, Cricetidae). Journal of Mammalogy 98: 1010–1026. https://doi.org/10.1093/jmammal/gyx074

Phillips MJ (2009) Branch-length estimation bias misleads molecular dating for a vertebrate mitochondrial phylogeny. Gene 441(1–2): 132–140. https://doi.org/10.1016/j.gene.2008.08.017

Posada D (2008) jModelTest: phylogenetic model averaging. Molecular biology and evolution 25(7): 1253–1256. https://doi.org/10.1093/molbev/msn083

Pousargues E (1896) Note sur une espéce asiatique du genre *Zapus* (Coues). Annales des Sciences Naturelles 8(1): 220.

Ronquist F, Huelsenbeck JP (2003) MrBayes 3: Bayesian phylogenetic inference under mixed models. Bioinformatics 19(12): 1572–1574. https://doi.org/10.1093/bioinformatics/btg180

Shenbrot G, Bannikova A, Giraudoux P, Quere J, Raoul F, Lebedev V (2017) A new recent genus and species of three-toed jerboas (Rodentia, Dipodinae) from China: A living fossil?. Journal of Zoological Systematics and Evolutionary Research 55(4): 356–368. https://doi.org/10.1111/jzs.12182

Smith AT, Xie Y (2008) A guide to the mammals of China. Princeton University Press. Princeton, New Jersey, 135–144.

Song YG, Fang XM, Torii M, Ishikawa N, Li JJ, An ZS (2007) Late Neogene rock magnetic record of climatic variation from Chinese eolian sediments related to uplift of the Tibetan Plateau. Journal of Asian Earth Sciences 30: 324–332. https://doi.org/10.1016/j.jseaes.2006.10.004

Sui LL, Cheng JL, Xia L, Yang QS (2022) Phylogeny and distribution patterns of Dipodoidea in China. Acta Theriologica Sinica 42(2): 131–143. https://doi.org/10.16829/j.slxb.150616

Tamura K, Peterson D, Peterson N, Stecher G, Nei M, Kumar S (2011) MEGA5: molecular evolutionary genetics analysis using maximum likelihood, evolutionary distance, and maximum parsimony methods. Molecular biology and evolution 28(10): 2731–2739. https://doi.org/10.1093/molbev/msr121

Tamura K, Stecher G, Peterson D, Filipski A, Kumar S (2013) MEGA6: Molecular Evolutionary Genetics Analysis version 6.0. Molecular biology and evolution 30(12): 2725–2729. https://doi.org/10.1093/molbev/mst197

Thomas O (1912) On a collection of small mammals from the Tsin-ling Mountains, Central China, presentedby Mr. G. Fenwick Owen to the National Museum. The Annals and Magazine of Natural History 8.10(58): 402. https://doi.org/10.1080/00222931208693252

Wan T, He K, Jin W, Liu SY, Chen ZZ, Zhang B, Jiang, XL (2018) Climate niche conservatism and complex topography illuminate the cryptic diversification of Asian shrew-like moles. Journal of Biogeography 45: 2400–2414. https://doi.org/10.1111/jbi.13401

Wei F, Costanza R, Dai Q, Stoeckl N, Gu X, Farber S, Zhang W (2018) The value of ecosystem services from Giant Panda reserves. Current Biology 28: 2174–2180 [e7]. https://doi.org/10.1016/j.cub.2018.05.046

Wei FW, Yang QS, Wu Y, Jiang XL, Liu SY (2022) Taxonomy and distribution of Mammals in China. Science Press.

Wilson DE, Mittermeier RA (2018) Handbook of the Mammals of the World: True Mice and Rats Gerbils and Relatives. Barcelona: Lynx Edicions.

Yang Z, Rannala B (2010) Bayesian species delimitation using multilocus sequence data. Proceedings of the National Academy of Sciences of the United States of America 107(20): 9264–9269. https://doi.org/10.1073/pnas.0913022107

Yang FS, Qin AL, Li YF, Wang XQ (2012) Great genetic differentiation among populations of Meconopsis integrifolia and its implication for plant speciation in the Qinghai-Tibetan Plateau. PLoS ONE 7(5): e37196. https://doi.org/10.1371/journal.pone.0037196

Yu G, Zhang M, Rao D, Yang J (2013) Effect of Pleistocene climatic oscillations on the phylogeography and demography of red knobby newt (Tylototriton shanjing) from southwestern China. PLoS ONE8(2): e56066. https://doi.org/10.1371/journal.pone.0056066

Zhang B, He K, Wan T, Chen P, Sun G, Liu SY, Nguyen TS, Lin LK, Jiang XL (2016) Multi-locus phylogeny using topotype specimens sheds light on the systematics of Niviventer (Rodentia, Muridae) in China. BMC Evolutionary Biology 16: 261. https://doi.org/10.1186/s12862-016-0832-8

Zheng Y, Rui P, Masaki KO, Zeng X (2011) Exploring patterns and extent of bias in estimating divergence time from mitochondrial DNA sequence data in a particular lineage: A case study of salamanders (order Caudata). Molecular Biology and Evolution 28(9): 2521–2535. https://doi.org/10.1093/molbev/msr072

Supplementary material 1

Supplementary file

Authors: Siyu Yang, Fei Xie, Chengxin Zhou, Zongyun Zhang, Xuming Wang, Shaoying Liu, Shunde Chen

Data type: docx

Explanation note: **table S1.** Primers used for PCR and sequencing used in this study; **table S2.** Sampling information including localities and GenBank accession numbers from GenBank in this study; **table S3.** The best molecular evolution model used in phylogenetic reconstructions based on jModeltest; **table S4.** Result of BPP species delimitation based on CYT B+nuDNA and nuDNA dataset; **table S5.** Cranial measurements of the genus *Eozapus* used in this study.

Copyright notice: This dataset is made available under the Open Database License (http://opendatacommons.org/licenses/odbl/1.0/). The Open Database License (ODbL) is a license agreement intended to allow users to freely share, modify, and use this Dataset while maintaining this same freedom for others, provided that the original source and author(s) are credited.

Link: https://doi.org/10.3897/zse.101.133734.suppl1